

Mussel-inspired conductive Ti₂C-cryogel promotes functional maturation of cardiomyocytes and enhances repair of myocardial infarction

Genlan Ye^{1,3#}, Zubiao Wen^{2#}, Feng Wen¹, Xiaoping Song¹, Leyu Wang¹, Chuangkun Li¹, Yutong He^{1,3}, Sugandha Prakash¹, Xiaozhong Qiu^{1*}

¹Guangdong Provincial Key Laboratory of Construction and Detection in Tissue Engineering, School of Basic Medical Science; Biomaterials Research Center, School of Biomedical Engineering, Southern Medical University, Guangdong, Guangzhou 510515, China

²College of Chemistry and Chemical Engineering, Jiangxi Normal University, Nanchang 330022, China

³Guangzhou Regenerative Medicine and Health Guangdong Laboratory, Guangzhou 510005, China

These authors contributed equally to this work.

***Corresponding author:**

Prof. Xiaozhong Qiu

Guangdong Provincial Key Laboratory of Construction and Detection in Tissue Engineering, School of Basic Medical Science, Southern Medical University, Guangdong, Guangzhou 510515, China

Email address: qqiu_xzh@163.com

Telephone number: 86-20-61648401

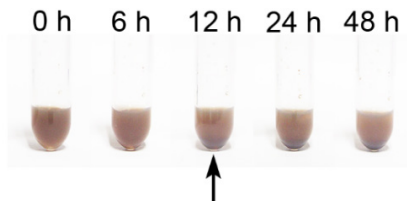


Figure S1. Graphene-cryogel prepolymer solutions rest for different times.

Arrow showed aggregation occurred in 12 hours.

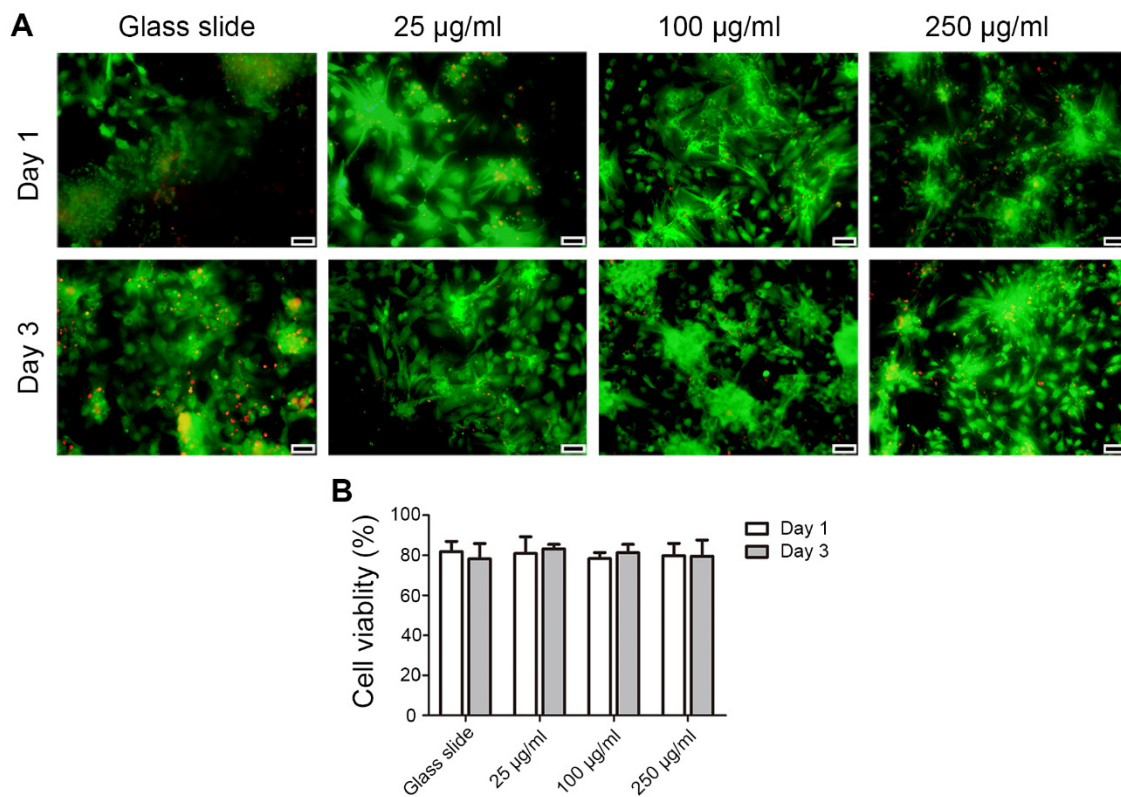


Figure S2. Biocompatibility of the MXene Ti_2C nanoparticles. A) Live-dead staining for neonatal rat CMs treated with various concentrations of Ti_2C nanoparticles on day 1 and day 3 of treatment. B) Quantitative cell viability of CMs based on the live-dead staining. Green cells represented live cells and red cells represented dead cells. Scale bars = 50 μm .

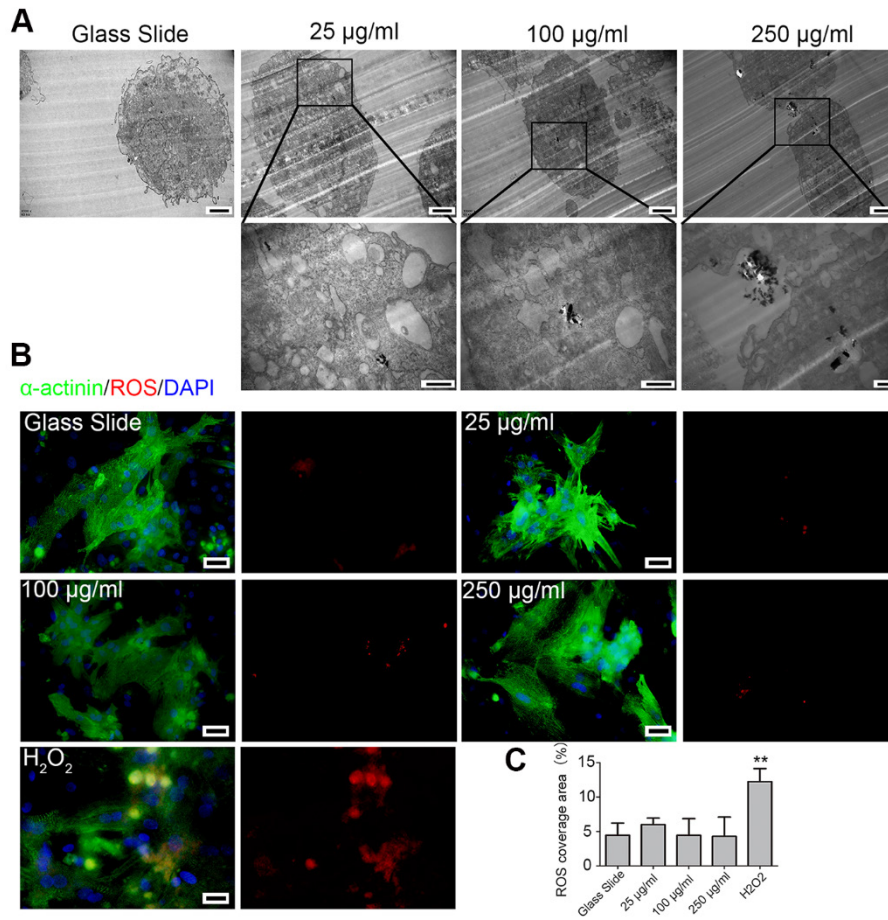


Figure S3. A few of Ti_2C nanoparticles invaginated into the CMs and did not elevate the cellular ROS levels. A) TEM of the CMs treated with different concentrations of Ti_2C nanoparticles. B) Fluorescence images of the ROS in CMs treated with a different concentration of Ti_2C nanoparticles. C) The quantification of the ROS level.

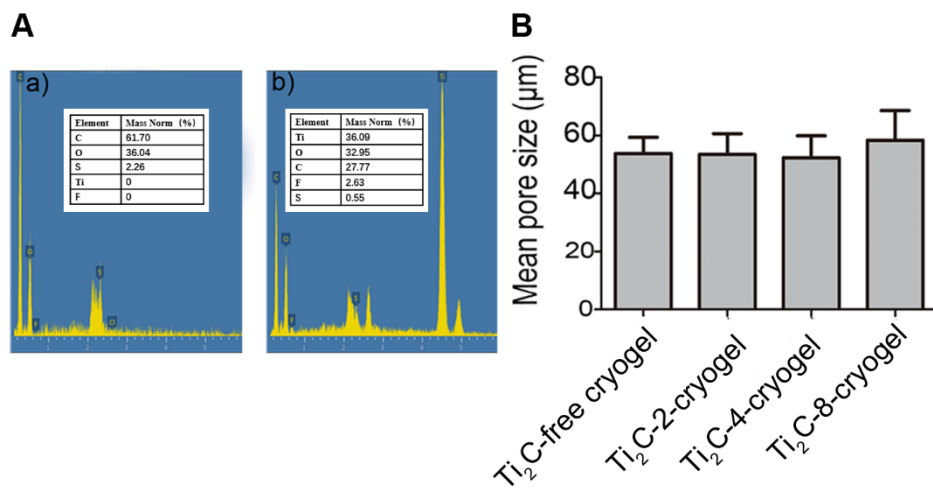


Figure S4. The characteristic of the Ti₂C cryogel. A) Element mass analysis of Ti₂C-free cryogel and Ti₂C-8-cryogel using energy-dispersive X-ray spectroscopy analysis. B) Mean pore sizes of different cryogels.

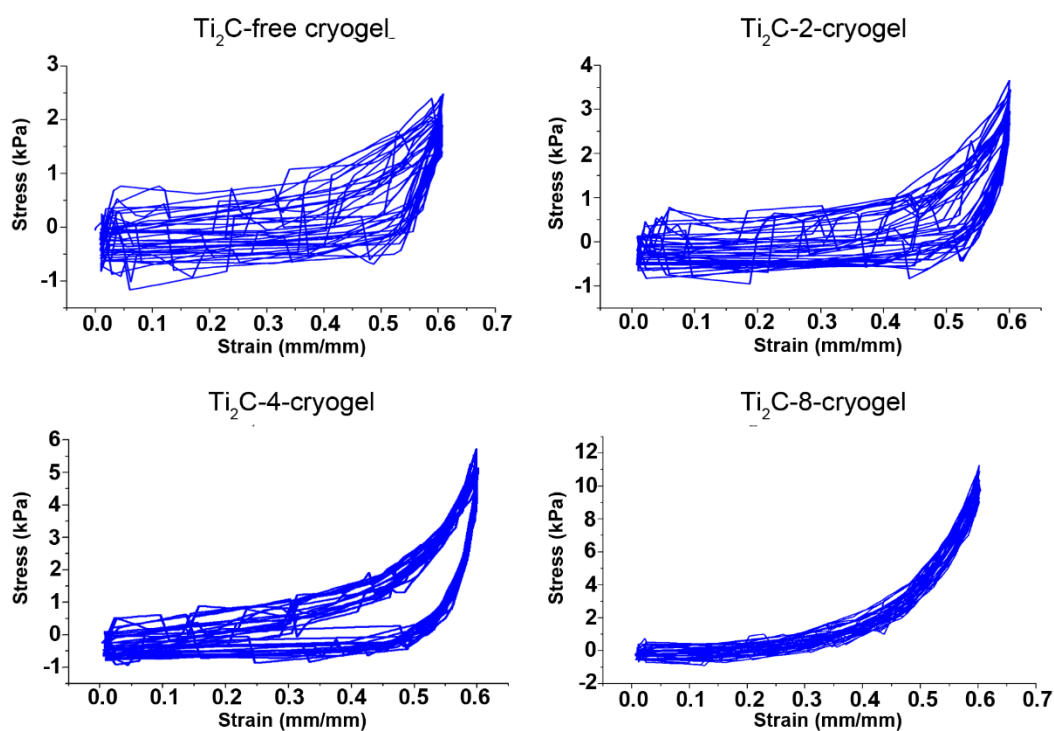


Figure S5. The stress-strain curve of different cryogels in compressive cycling test up to 60 % deformation for the first 20 cycles.

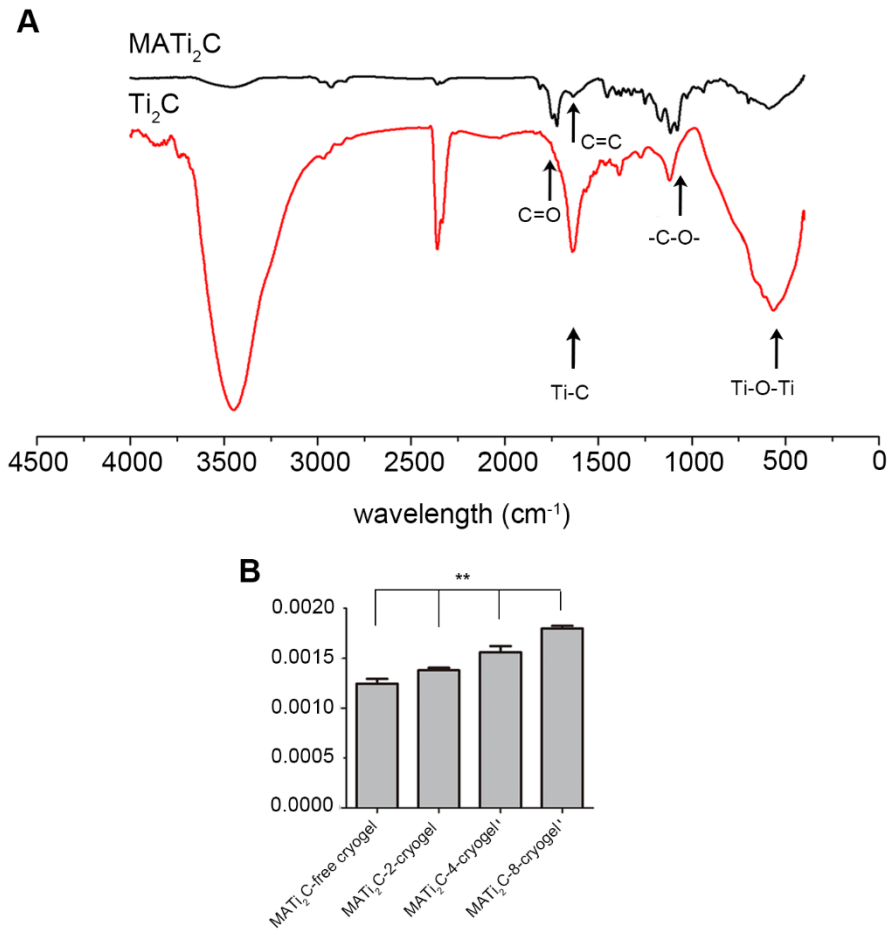


Figure S6. Characterization of MATi₂C and MATi₂C-cryogel. A) FTIR spectrum of MATi₂C and Ti₂C nanoparticles B) Conductivities of different MATi₂C-cryogels detected via four points probe method. n = 3. ***p* < 0.01

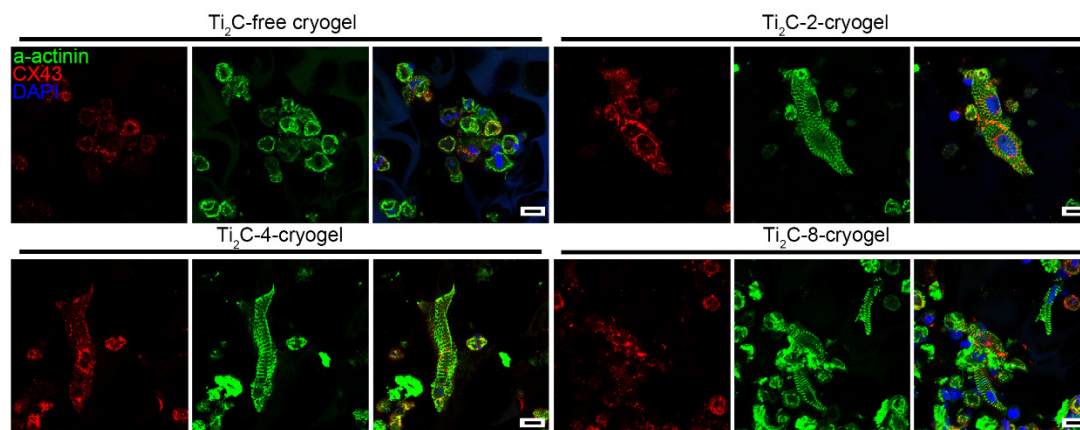


Figure S7. Immunofluorescent staining for cardiac-specific protein α -actinin (green) and CX43 (red) in CMs cultured on different Ti_2C -cryogels on day 3. Scale bars =10 μ m.

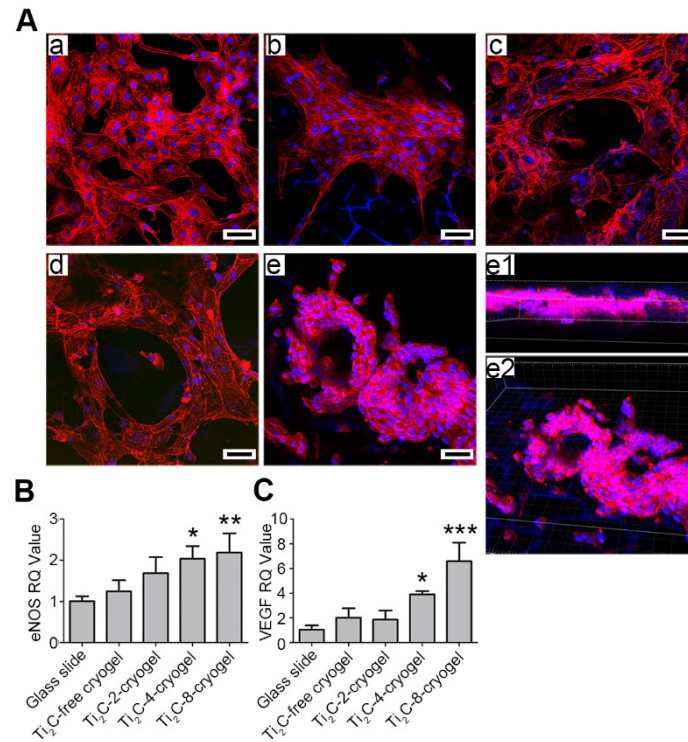


Figure S8. Ti₂C-cryogel promoted the tube formation of RAEC *in vitro*. A) F-actin showed the cell morphology of RAEC cultured on a glass slide or other different cryogels. 3D tube structure of RAEC formatted in Ti₂C-8-cryogels (a, glass slide, b, Ti₂C-free cryogel, c, Ti₂C-2-cryogel, d, Ti₂C-4-cryogel, e, Ti₂C-8-cryogel). B) and C) Expression of eNOS and VEGF genes in RAEC on a glass slide or other different cryogels. Scale bars=50 μ m. n=3 * p <0.05, ** p <0.01, *** p <0.001

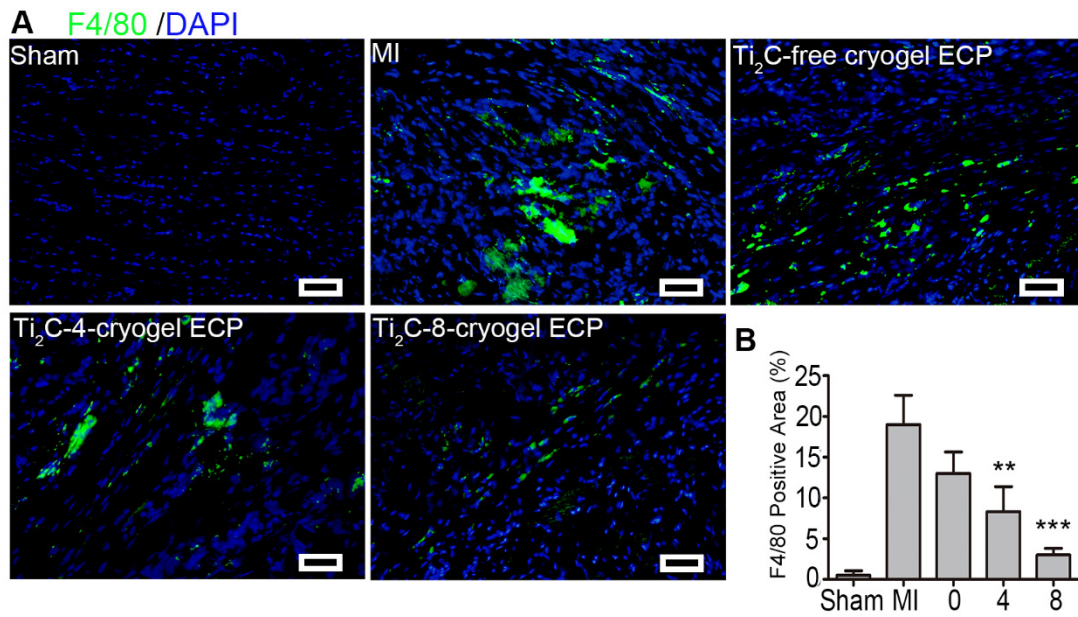


Figure S9. Inflammation of infarcted area after ECPs transplantation. A) F4/80 immunostaining in the infarcted area in different groups. B) F4/80-positive area in different groups. n = 3. ** $p < 0.01$, *** $p < 0.001$

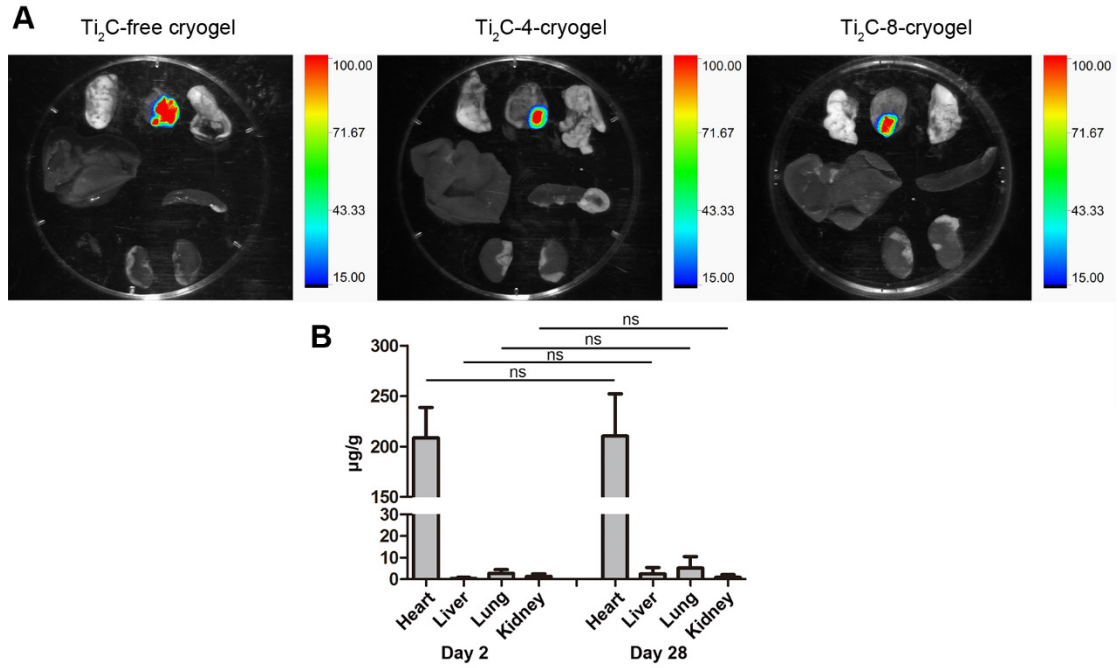


Figure S10. The location of the cryogel in rats and distribution of the Ti_2C nanoparticles in different organs in 28 days after transplantation. A) Fluorescence signals of cy5-labeled cryogels detected by a fluorescence imaging system. B) The total titanium content in different organs measured in 2 and 28 days after ECPs transplantation.

Supplemental movie 1. The compress and the release of the Ti₂C-8-cryogel;

Supplemental movie 2. The calcium transient in CMs cultured on different ECPs for 3 days;

Supplemental movie 3. The synchronous contraction of different ECPs *in vitro* on day 7 under the microscope;

Supplemental movie 4. The synchronous contraction of Ti₂C-8-cryogel ECP *in vitro* on day 7 observed by naked eyes.

Supplemental movie 5. The short-axis B model echo video of the ECP transplantation group.